



Effect of hydrodynamic characteristics on the performance of biofilm for degrading phenol in inverse fluidized bed biofilm reactor

S. Sabarunisha Begum*, K.V. Radha

Department of Chemical Engineering, A.C. College of Technology, Anna University, Chennai 600 025, India, Tel. +91 44 22359124; Fax: +91 44 2715 6640; emails: sabarunisha@gmail.com (S. Sabarunisha Begum), radhavel@yahoo.com (K.V. Radha)

Received 23 August 2013; Accepted 22 May 2014

ABSTRACT

The influence of some hydrodynamic effects on the performance of biofilm in inverse fluidized bed biofilm reactor (IFBBR) was studied with low-density polystyrene support particles of various sizes (2.9, 3.5, and 3.8 mm) using *Pseudomonas fluorescens* for the degradation of phenol. The biofilm reactor was operated under different superficial air velocities for a fixed settled bed height of particles to study the effect of hydrodynamics on biofilm thickness, biofilm dry density, bioparticle density, and attached and suspended biomass concentrations for efficient biodegradation of phenol. There is evidence that the chemical oxygen demand reduction and phenol degradation efficiency were found to be high at the optimized superficial air velocity with controlled biofilm thickness and for a stable and dense biofilm dry density. The results of the study revealed that with increase in superficial air velocity, the biofilm thickness and bioparticle density decreases while the biofilm dry density and suspended biomass concentration increases. However, above a critical superficial velocity (optimal superficial velocity) the detachment force does not control the outgrowth of the biofilm anymore and the thickness increases rapidly with decreasing suspended biomass concentration. The optimal superficial velocity for better biodegradation of phenol was found to be 0.240, 0.220, and 0.230 m/s for the particle sizes of 2.9, 3.5, and 3.8 mm, respectively. The particle size of 3.5 mm has been found to be the optimal particle size for efficient biodegradation of phenol in IFBBR with better hydrodynamic effects and biofilm morphology.

Keywords: Hydrodynamics; Superficial air velocity; Biofilm; Inverse fluidized bed; Biodegradation

1. Introduction

Biofilm is a multispecies, immobilized cell community, and can be found in a wide range of different systems. The formation of biofilm is a multistep process, and physicochemical and biological factors are involved. None of the individual species in the biofilm

may be capable of completely degrading influent wastes. Complete degradation of industrial waste involves a complex series of interaction between the resident species. The morphological characteristics of biofilms (biofilm thickness, biofilm density, bioparticle density, and concentrations) are very important for the stability and performance of the biofilm [1]. These factors strongly affect the biomass hold-up and mass transfer in a biofilm reactor [2,3].

*Corresponding author.

Biofilm reactor has been frequently applied in wastewater treatment. The feasibility and efficiency of biofilm reactors for removing biodegradable matter, nitrogen, and phosphate from municipal and industrial wastewater have been shown [4–6]. Biofilm reactors are desirable in biological treatment processes because a very high number of highly concentrated organisms can be maintained and treated in the reactor which takes up a small amount of space. In biological biofilm reactors, the detachment force resulting from hydrodynamic shear and/or particle–particle collision is a key factor that influences the formation, structure, and stability of biofilms under hydrodynamic conditions. The detachment force has significant influence on the structure, mass transfer, production of exopolysaccharides, and metabolic and genetic properties of the biofilm [7]. In biofilm systems, a higher detachment force would result in a stronger biofilm, however, biofilm tends to become heterogeneous, porous, and weaker structure when the detachment force is weak [8–11]. Moreover, thinner biofilms obtained under higher shear stress are more stable and have a higher active biomass concentration, leading consequently to higher biofilm activity that is the key parameter for an optimized bioreactor operation [12]. Thus, the performance and stability of the biofilm reactor depends on the structure of the biofilm formed around the support.

So far, it has been recognized that the detachment force associated mechanisms are still unclear in the formation of biofilm. In an engineering sense, the detachment forces can be manipulated, as a control parameter, to produce a more stable and compact biofilm for use in wastewater treatment. Thus, optimization of hydrodynamic conditions in relation to detachment forces is necessary in future engineering design of biofilm reactors. Therefore, this paper attempts to study and optimize the effect of hydrodynamic detachment force (superficial velocity) on the structure and behavior of biofilm in degrading phenol in a three phase inverse fluidized bed biofilm reactor (IFBBR) and to discuss how biofilm respond to detachment force under hydrodynamic conditions.

In this study, the hydrodynamic characteristic influence on biofilm performance in IFBBR for the degradation of synthetic phenolic wastewater using *Pseudomonas fluorescens* is examined. The characteristics of biofilm attached to solid support particles of various sizes and its performance studies at different hydrodynamic conditions are evaluated for efficient phenol degradation. The biofilm characteristics (biofilm thickness, biofilm dry density, and attached dry biomass concentration) have been studied as a function of superficial air velocity (detachment force) and

phase hold-ups. Hydrodynamic effects with better biofilm morphology have been optimized for efficient biodegradation of phenol in IFBBR.

2. Materials and methods

2.1. Micro-organism and culture medium

The micro-organism *P. fluorescens* (MTCC103) was chosen for biofilm development over the support particles in IFBBR which has the potential to degrade phenol using it as the sole carbon and energy source. The preliminary stage of upstream processing work started with reviving the host by subsequent streaking of a mother culture of *P. fluorescens* on a *Pseudomonas* agar slant and keeping it for incubation at 28°C for 2 d [13,14]. A primary culture was prepared by transferring two loops full of micro-organisms having concentration of 4.1×10^4 colonies/ml from the agar slant into 100 ml of feed medium containing 20 ml of mineral salt medium [15] and 80 ml of phenol (substrate) of concentration 1,200 mg/l in four 250 ml conical flasks. They were kept in a shaker incubator at a temperature of 28°C and agitated at a speed of 120 rpm until it attained an exponential increase in the concentration of cell mass during its log phase (steady state growth). Once the microbe has attained a steady state of growth, 10 ml of the primary culture was transferred into four 250 ml conical flasks, each containing 100 ml of the feed medium, and the incubation process was repeated. These were the secondary cultures used as inoculum for biofilm development over the support particle in IFBBR before the biodegradation process and was done to adapt the microbe to that particular substrate concentration. Air was supplied at superficial air velocity ranging between 0.216 and 0.244 m/s which was sufficient for biomass growth. The initial pH of the feed medium was 6.5 and the temperature was at 28°C.

2.2. Support particles

Low-density non-porous polystyrene beads of various sizes were used as support media (support particle). Some physical characteristics of the support particles are summarized in Table 1.

2.3. Experimental setup and reactor configuration

IFBBR is a tubular reactor constructed from the Duran glass with height to diameter (H:D) ratio of 10:1. The overall height of the reactor was 105 cm and the diameter was 10 cm. The height of the inner draft tube was 70 cm long and fixed at a height of 15 cm

Table 1
Physical characteristic of the support particles

Physical properties	Particle diameter (mm)		
	2.9	3.5	3.8
Mass of single particle, mg	6.5	17	20
Volume of single particle, 10^{-3} cm^3	10.45	19.7	21.6
Density of particle, kg/m^3	619	863	926
Surface area, cm^2	0.2463	0.3631	0.4071
Surface area to volume ratio, cm^2/cm^3	20.68	17.14	16.60

from the bottom of the reactor. The diameter of the draft tube was 5 cm. A mesh was placed at a height of 10 cm from the bottom of the draft tube to improve phase mixing. A converging–diverging conical insert was placed just above the draft tube to eliminate dead zones near the reactor wall and to avoid particle accumulation above the liquid level. The working volume of the reactor was 5.6 l (Fig. 1). The ports were provided at the top and bottom of the reactor for liquid recirculation and air inlet, respectively. Two spargers, one at the bottom (to prevent settling of particles) and the other at the side of the conical bottom (for fluidizing the bioparticles) were connected to their respective air pumps (Model HS1), and a valve to control the air flow rate. A peristaltic pump (Model RH-120S) was used for controlling the recycle liquid flow rate.

2.4. Experimental procedure

IFBBR was operated with 5.6 l of feed medium having phenol concentration of 1,200 mg/l as synthetic

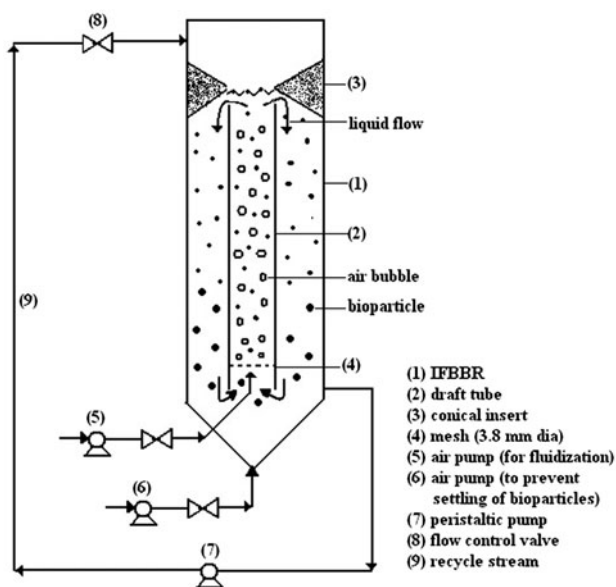


Fig. 1. Schematic representation of IFBBR setup.

effluent for different experimental runs of varying superficial air velocities. Polystyrene support particles of various diameters (3.8, 3.5, and 2.9 mm) were immersed into the feed medium inside the reactor during different experimental runs. The support particles were weighed accurately and filled inside the reactor for a fixed ratio of settled bed height volume to reactor working volume, $(V_b/V_r)_{\text{opt}}$ of 0.2 which has the settled bed height $(H_s)_{\text{opt}}$ value of 17.87 cm in the reactor [16].

The reactor was allowed to run for 3–4 d with feed medium having phenol concentration of 1,200 mg/l for the effective formation of biofilm over support particles. The biofilm formed on the support particle was identified by the conventional staining techniques. The gram's stain was used to identify the formation of biofilm by gram negative rod shaped bacteria (*P. fluorescens*). The viability check was performed using trypan blue staining. After the formation of biofilm onto support particles, a fresh supply of the feed medium having phenol concentration of 1,200 mg/l was fed into IFBBR for the biodegradation process. During the biodegradation process, pH was slightly increased from 6.5 to 6.8 with the degradation of phenol, since it is a weak acid and tends to become slightly alkaline due to the formation of base phenoxide ion in its hydrolytic pathway reaction mechanism. The pH of the feed medium was thus maintained and self-controlled within the optimal growth limit of the organism in the reactor [17].

Recycling of liquid was brought about with a minimum flow rate of 40 ml/min which increases the homogenization of the solution and prevents stagnant regions inside the reactor [18]. The reactor began foaming at the initial hours of biomass inoculation into the reactor. A similar type of foaming has been observed by other researchers during biodegradation of phenol [19]. The foam was very thick and dense and did not collapse, and it entrapped some bioparticles (particles covered by biofilm). Eventually, it was determined that foaming greatly decreased if the biomass at the bottom of the reactor was not allowed to

settle [20]. An air sparger connected with an air pump at the bottom of the reactor prevents the settling of bioparticles and reduces foam formation in the IFBBR. The reactor was operated with continuous gas (air) flow and with batch liquid and solid phases under non-sterile conditions.

2.5. Flow regimes

Phase mixing was studied visually by observing the solid, liquid, and gas phases in IFBBR [21]. Once the low-density solid support particles were fed to the reactor, they form a packed bed like appearance at the top of the column. As the gas velocity is increased, first, the bottom layer of the packed bed starts fluidizing. With further increase in gas velocity, the rest of the bed fluidizes and the bed begins to expand downwards. When the gas velocity reaches the minimum fluidization velocity, the pressure drop across the bed attains the maximum. At this point, the entire bed is in fluidization condition but the concentration of solid particles is not uniform throughout the bed. With further increase in gas velocity, there will be uniform concentration of solid particles throughout the reactor and the velocity is termed as critical fluidization velocity [22]. Experiments were carried out at various superficial air velocities, U_g , which are just equal to or larger than the critical fluidization velocity below which the fluidization of particles was not uniform throughout the reactor.

2.6. Measurement and analysis

Experiments were carried out to determine the effect of hydrodynamic characteristics on the performance of biofilm and biomass for the degradation of phenolic effluent. Support particles of varying diameter (2.9, 3.5, and 3.8 mm) were used in different experimental runs for various superficial velocities, U_g , and the optimum size of the support particle was determined for the better hydrodynamic effects and higher degradation efficiency of phenol. Superficial gas velocity was varied as 0.236, 0.240, and 0.244 m/s for 2.9 mm, 0.216, 0.220, and 0.224 m/s for 3.5 mm, and 0.226, 0.230, and 0.234 m/s for 3.8 mm diameter support particles and the optimum superficial velocity was determined for each media (support particle) size for effective biodegradation of phenol.

Samples were collected at regular intervals to estimate the phenol concentration, biomass concentration (suspended and attached), biofilm dry density, bioparticle density, biofilm thickness, chemical oxygen demand (COD), gas hold-up, and pH. The reactor was

allowed to run continuously till the analytical techniques showed that phenol was completely degraded. All determinations were performed according to standard procedures and methods [23]. Phenol concentration was analyzed using the standard aminoantipyrine method with absorbance measurements at 510 nm spectrophotometrically [24]. Suspended biomass concentration was determined by dry weight [25] whereas the attached biomass concentration was measured by the increase of attached volatile solids on polystyrene support particles. The particles covered by biofilm (40–50 bioparticles) were taken out from the top portion of the reactor; air dried at 110°C for 2 h and their dry weight (the attached volatile solid) was found out. The difference between the initial weight of support particles and the bioparticles was considered as the attached biomass weight and was expressed as (g_{AVS}/g_{solid}) [26,27]. The biofilm dry density and thickness of the biofilm were determined as calculated by Rabah et al. and Zhang et al. from the net dry biomass weight of the bioparticle [27,28].

The following equations have typically been used to determine the volume fraction (hold-up) of all phases and pressure drop per unit height in the three phase inverse fluidized bed [29].

$$(\varepsilon_g + \varepsilon_s + \varepsilon_l) = 1 \quad (1)$$

$$\varepsilon_s = \frac{M_s}{(H_s A \rho_s)} \quad (2)$$

where ε_g , ε_{sr} and ε_l are gas, liquid, and solid hold-ups, respectively, ρ_g , ρ_{sr} and ρ_l similarly represent densities, g is acceleration due to gravity. From Eq. (1) it is evident that high-density particles lead to high-pressure drop causing increase in power consumption. Thus, the application of low-density particles in IFBBR with draft tube arrangement can minimize this tendency [30].

The average phase hold-ups are measured by the following relation:

$$\varepsilon_s = \left(\frac{V_s}{V_r} \right) \quad (3)$$

$$\varepsilon_g = \frac{(Z_f - Z_i)}{Z_f} \quad (4)$$

where V_s and V_r are volume of solid particles and working volume of the reactor, respectively, Z_f and Z_i are the aerated liquid level in the reactor column after fluidization and the initial liquid level before aeration, respectively.

3. Results and discussion

The degradation of phenol was carried in an IFBBR using *P. fluorescens*. Experiments were conducted to study the hydrodynamic effects on biofilm performance for better biodegradation of phenol with various particle sizes for different superficial air velocity. The optimum superficial velocity has been found out for each media size for better biofilm morphology and higher biodegradation effect. Optimum particle size was identified for better hydrodynamic effects on biofilm performance. All the experimental runs were done in triplicate and the error analysis was found to be 0.03%.

3.1. Biodegradation effect on various particle sizes at different superficial air velocities

Experiments were conducted for the support particles of various sizes at different superficial air velocities. Because of low density (619 kg/m^3) of the support particle compared with the liquid phase, the media size of 2.9 mm requires high-superficial air velocity for the inverse fluidization process when compared with other particle sizes in the reactor.

The biodegradation effect was determined by the COD values and phenol concentration measured at regular time intervals. Fig. 2 shows the variation of COD values with respect to biodegradation time for the particle sizes 2.9 mm (Fig. 2(a)), 3.5 mm (Fig. 2(b)), and 3.8 mm (Fig. 2(c)). The time taken for complete reduction of phenol was found to be 32, 48, and 52 h for the particle sizes 2.9, 3.5, and 3.8 mm, respectively. It was inferred that for smaller size particles, the surface area of the bioparticles increases thereby degrades phenol in lesser degradation time of 32 h. For larger particle sizes, the effective surface area of contact decreases and hence, overall time taken for phenol degradation increases. For a given media size, there exists one superficial velocity (optimum superficial velocity, U_{gm}) which facilitates more substrate diffusion in biofilms favoring higher biodegradation effect on phenol and COD removal efficiency.

From the Fig. 3, it is observed that optimum superficial velocity (U_{gm}) for 2.9, 3.5, and 3.8 mm of particles was found to be 0.240, 0.220, and 0.230 m/s, respectively for better biodegradation of phenol and the final COD removal efficiency was found to be 98.7, 98.5, and 97.8%, respectively. Fig. 4 shows the variation of COD removal efficiency (%) at the optimized superficial velocity (U_{gm}) for various particle sizes. The media size suited well for the industrial application should require low-superficial air velocity resulting in higher biodegradation efficiency. Experimentally, it was identified that particle size of 3.5 mm diameter was

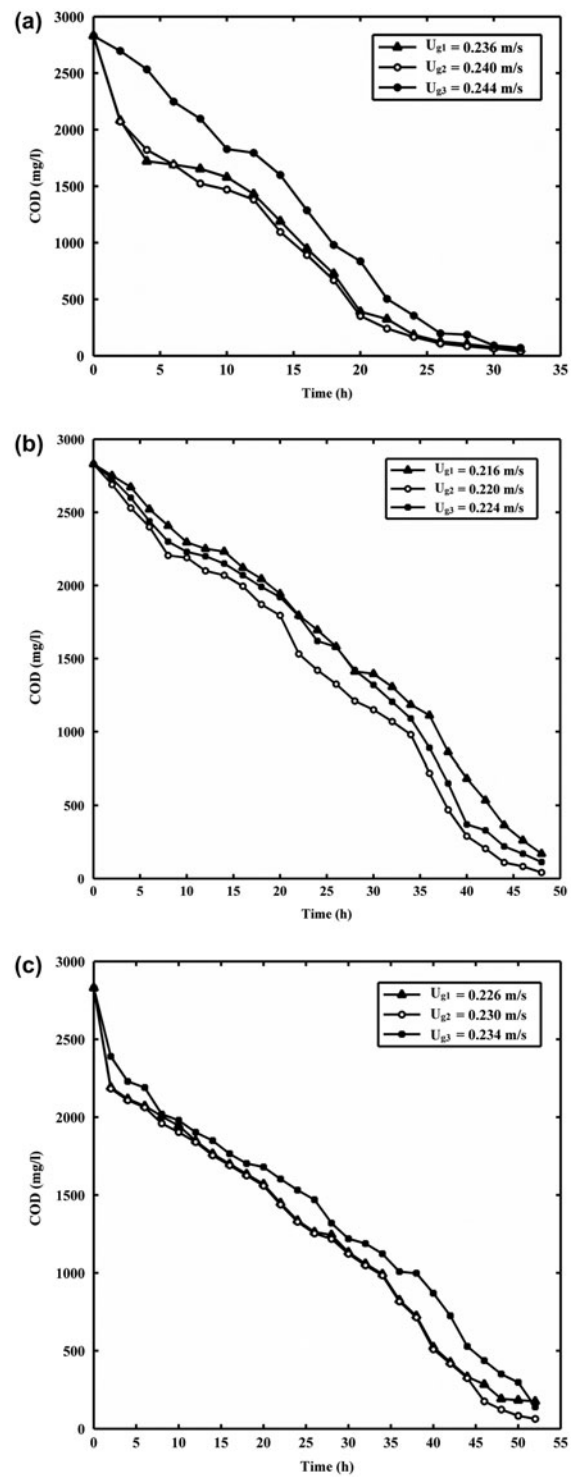


Fig. 2. Variation of COD with biodegradation time for the particle size 2.9 mm (a), 3.5 mm (b), and 3.8 mm (c).

found to be the optimum media size which required lower optimal superficial air velocity of 0.220 m/s for degrading the synthetic phenolic effluent from the

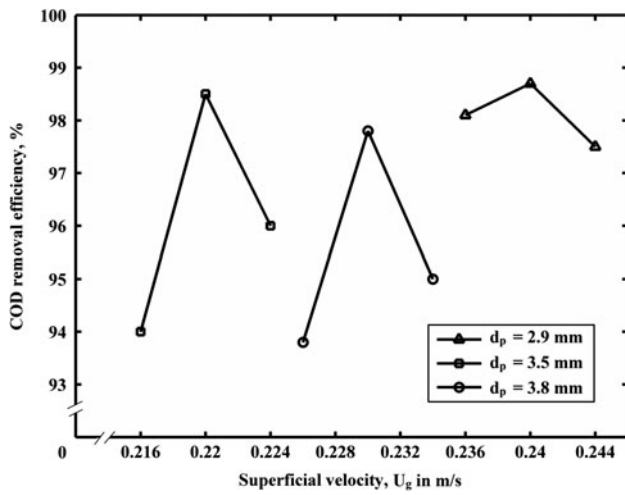


Fig. 3. Effect of superficial velocity, U_{gr} on COD removal efficiency (%) for various media sizes.

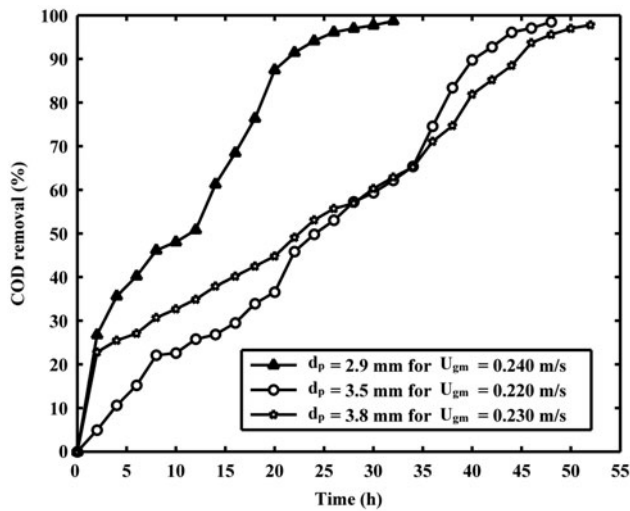


Fig. 4. Variation of COD removal efficiency (%) at the optimized superficial velocity (U_{gm}) for various particle sizes.

initial COD value of 2,830–42 mg/l with 98.5% removal efficiency.

3.2. Biofilm characteristics on various particle sizes for the optimized superficial air velocity

3.2.1. Biofilm thickness and biofilm dry density

The maintenance of biofilm thickness could have been the crucial factor for the complete degradation of

phenol. Biofilm thickness and biofilm dry density were evaluated for the optimized superficial velocity of various particle sizes. Figs. 5 and 6 show the biofilm development and biofilm dry density at different time intervals. Biofilm dry density is a function of biofilm thickness. Biofilm development was found to be increasing initially due to the attachment of biomass on to support particles and then decreases due to the detachment of biomass during its dispersion stage. Increase in biofilm thickness shows less dense biofilm due to the formation of loose filamentous organisms resulting in decrease in biofilm dry density [9]. Biofilm

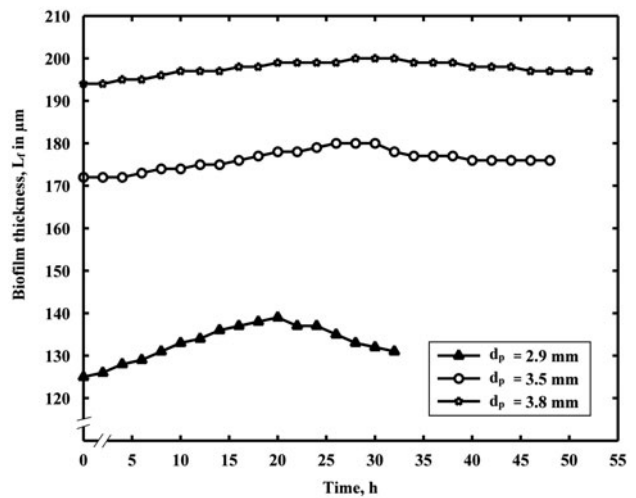


Fig. 5. Variation of biofilm thickness (L_f) development with time for various particle sizes at the optimized superficial air velocity U_{gm} .

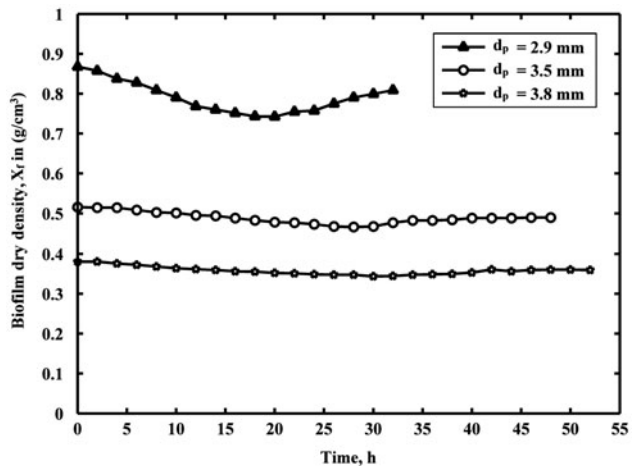


Fig. 6. Variation of biofilm dry density (X_f) with time for various particle sizes at the optimized superficial air velocity U_{gm} .

thickness decreases with media size. For smaller media size, the maintenance of thinner biofilms in IFBBR offers advantage of preventing biomass carry-over at high-superficial velocities. Thinner biofilm in IFBBR contributed to higher COD removal efficiency since they are more stable and dense whereas thicker biofilms are less stable and have low-biofilm dry density.

3.2.2. Suspended and attached biomass concentration

Suspended biomass is the free microbial cells grown on bulk substrate liquid and those which detached from the biofilm during its dispersion stage. Attached biomass is the dry weight of the biofilm attached over the bioparticle per unit weight of the support particle. Figs. 7 and 8 show the relationship between biomass (suspended and attached) concentrations for various sizes of support particles and time for the optimized superficial air velocity.

From Fig. 7, it was found that suspended biomass concentration increased for short time duration due to the adaption of the environment and then it started decreasing in the bulk liquid due to the attachment and formation of mature irreversible biofilms over support particle. It then again increased due to the attrition of biofilm in its dispersion stage of biofilm formation. The average suspended biomass concentration was found to be 0.778, 0.462, and 0.357 g/l for 2.9, 3.5, and 3.8 mm particle sizes, respectively. Thus, the suspended biomass concentration decreased with increasing support particle size which had thicker biofilms, whereas it increased for smaller particle size

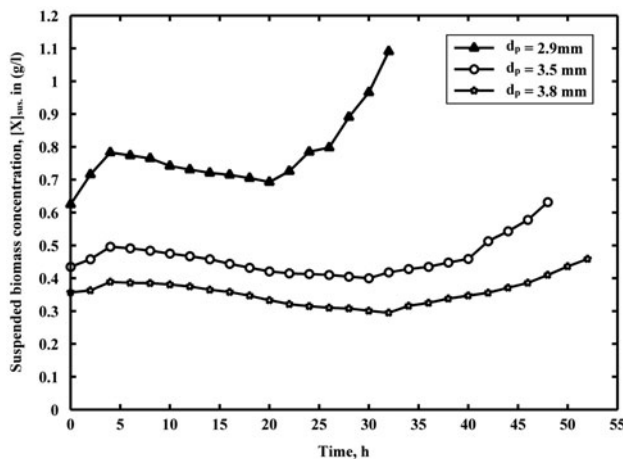


Fig. 7. Variation of suspended biomass concentrations with time for various particle sizes at the optimized superficial air velocity U_{gm} .

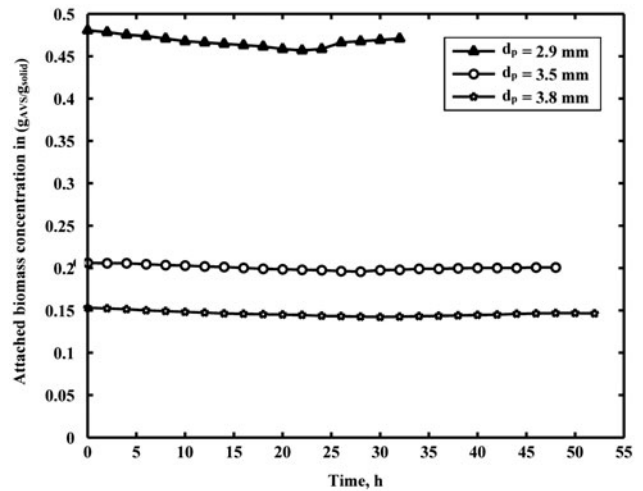


Fig. 8. Variation of attached biomass concentrations with time for various particle sizes at the optimized superficial air velocity U_{gm} .

having thin biofilms. It was found that even with the decrease in suspended biomass concentration over the period of the biodegradation process (from time $t = 5$ – 20 h), the COD values decreased proportionally with decreasing phenol concentration in the reactor which could only be due to the well adapted, constantly thickness maintained, and highly tolerated biofilm culture to higher concentration of phenol [31].

Attached biomass decreased initially due to the formation of less dense biofilm onto support particles and later on it increased due to the formation of stable and dense biofilm. Attached biomass concentration was found to be high for smaller particle size as it had thin stable dense biofilm and was found to be low for larger support particle sizes having thick but less stable biofilm (Fig. 8).

3.3. Effect of superficial velocity (detachment force) on biofilms

3.3.1. Biofilm thickness and biofilm dry density

The major detachment force present in a biofilm reactor results from the superficial velocity (fluidizing shear force) or particle–particle attrition; and has been considered as one of the most decisive factors in the formation of biofilm under hydrodynamic conditions. Fig. 9 shows the effect of superficial velocity on biofilm thickness (average of the sample points) for various particle sizes. Biofilm thickness decreases with superficial velocity due to high-detachment force exerted on the bioparticles until it reaches the optimum superficial velocity which produce compact and

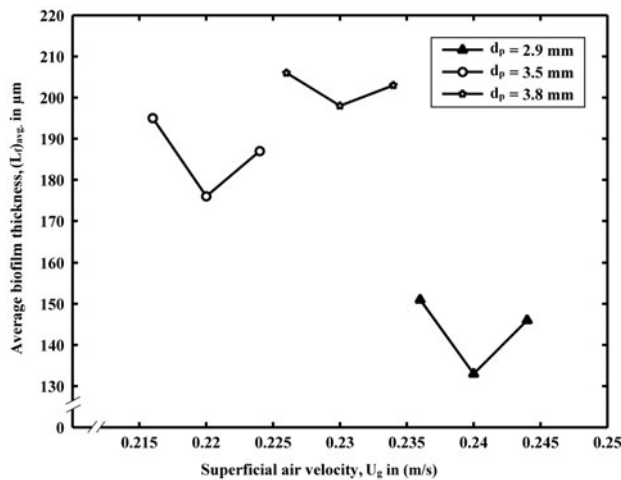


Fig. 9. Effect of superficial velocity on biofilm thickness (average of the sample points) for various particle sizes.

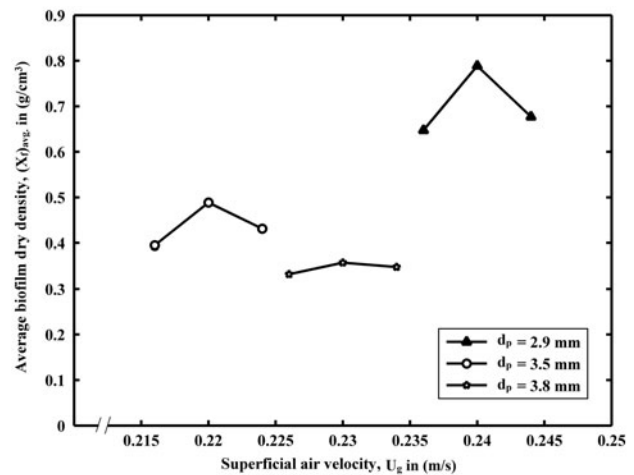


Fig. 10. Effect of superficial velocity on biofilm dry density (average of the sample points) for various particle sizes.

stable biofilm structure, then again increases where the detachment force does not control the outgrowth of biofilm anymore and the growth of the biofilm was found to be higher than the detachment from the surface [32]. The higher detachment force removes fluffy and less dense newly grown biomass on the outer layers of the particles [33]. Small size particle produces high-collision frequency due to more number of particles loaded inside the reactor for a fixed bed height. This resulted in lesser biofilm thickness coated onto small size particles whereas it increases for larger size particles [34]. There exists an optimum superficial velocity where the biofilm thickness was found to be less irrespective of particle sizes and the equilibrium biofilm thickness and biofilm dry density can be attained at an optimal superficial velocity. The optimum superficial velocity (U_{gm}) for 2.9, 3.5, and 3.8 mm of particles was found to be 0.240, 0.220, and 0.230 m/s, respectively, where the average biofilm thickness was found to be less and have smooth, stable, and denser biofilm. The average biofilm thickness, $L_{f,avg}$, was found to be in the range of 133–151 μm for the media size of 2.9 mm, 176–195 for the media size of 3.5 mm, and 198–206 for the media size of 3.8 mm.

Fig. 10 shows the effect of superficial velocity on biofilm dry density (average of the sample points) for various particle sizes. The biofilm dry density is a function of biofilm thickness. Bioparticles with lesser biofilm thickness produce more stable and highly dense biofilm (higher biofilm dry density) due extra biomass growth (in the form of microcolonies) in the base biofilm whereas the bioparticles with thicker biofilm have lower biofilm dry density. The average biofilm dry density, $X_{f,avg}$, was found to be increasing

with superficial velocity, U_g , then again decreases. Smaller the particle size produces highly dense biofilm than larger particle size due to the maintenance of thinner biofilm. The average biofilm dry density, $X_{f,avg}$, was found to be in the range of 0.6472–0.7886 g/cm^3 for the media size of 2.9 mm, 0.3949–0.4885 for the media size of 3.5 mm, and 0.3324–0.3579 for the media size of 3.8 mm.

3.3.2. Suspended and attached biomass concentration

Biomass concentrations were measured in terms of suspended and attached biomass concentrations. Suspended biomass is the free microbial cells grown on bulk substrate liquid and those which detached from the biofilm during its dispersion stage. Figs. 11 and 12 show the effect of superficial velocity on suspended and attached biomass concentrations (average of the sample points) respectively. The suspended biomass concentration increases with superficial velocity (the detachment force on bioparticles) till the optimum superficial velocity where most of the biofilm gets attrite from the bioparticles and gets suspended in the reactor and then decreases. The increase in suspended biomass concentration with increasing superficial velocity is far more significant when the biofilm is thinner [35]. The smaller diameter particle having thinner biofilm resulted in more suspended biomass concentration whereas the concentration decreases for larger size particles. The average suspended biomass concentration, $[X]_{\text{sus.avg},t}$ was found to be in the range of 1.229–1.271 g/l for particle size of 2.9 mm, 0.7245–0.8853 g/l for particle size of 3.5 mm, and 0.5219–0.7409 g/l for particle size of 3.8 mm (Fig. 11).

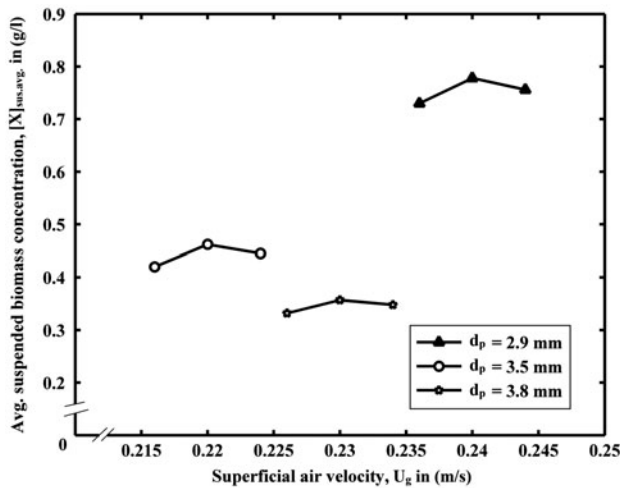


Fig. 11. Effect of superficial velocity on suspended biomass concentration (average of the sample points) for various particle sizes.

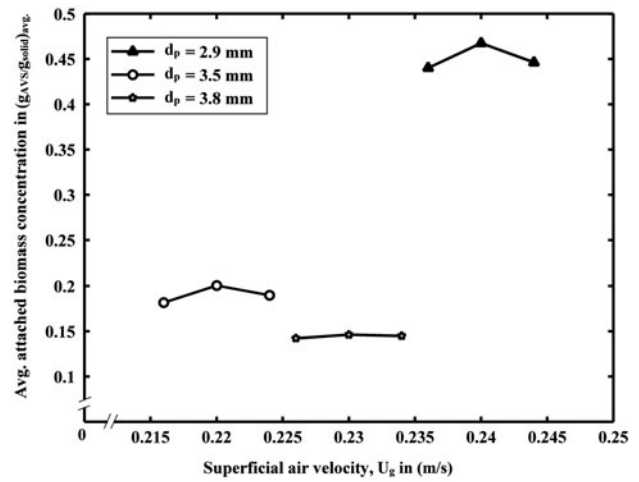


Fig. 12. Effect of superficial velocity on attached biomass concentrations (average of the sample points) for various particle sizes.

Attached biomass is measured from the dry mass of attached volatile solids per dry mass of the support particle, $(g_{\text{AVS}}/g_{\text{s}})_{\text{avg}}$. It increases with superficial velocity till the optimum and then decreases. Increase in superficial velocity produce thinner biofilms which are more stable, dense, and have higher dry density of the biofilm, which results in more dry mass of attached volatile solids. Smaller media size with thinner biofilm has more dry weight of attached solids than larger media size having thicker biofilm. Attached biomass concentration was found to vary from 0.4402 to 0.4676 g/g for particle size of 2.9 mm, 0.1816 to 0.2005 g/g for particle size of 3.5 mm, and 0.1422 to 0.1462 g/g for particle size of 3.8 mm (Fig. 12).

3.4. Effect of superficial velocity on phase hold-ups

Figs. 13 and 14 show the effect of superficial velocity on gas and solid hold-ups for different particle sizes. As the superficial velocity increases, the gas hold-up increases. Solid hold-up was found to be constant for a particular media size due to the occupancy of same volume of support particles in the fixed settled bed height. More number of particles has been utilized for smaller media size for a fixed settled bed height volume to reactor working volume ratio ($V_{\text{B}}/V_{\text{r}}$) whereas less for larger particle size. This results the solid hold-up decreasing with media size [36].

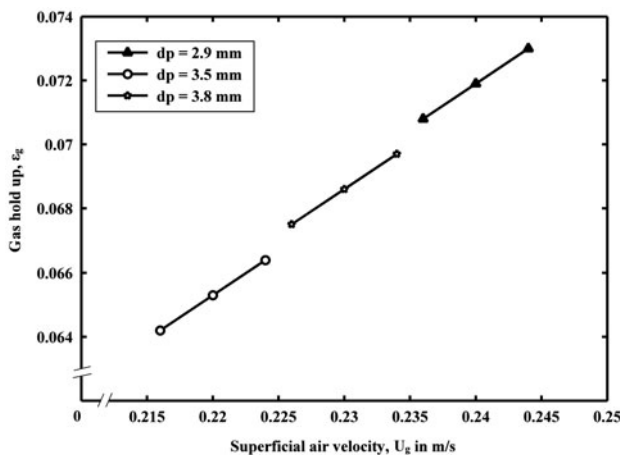


Fig. 13. Effect of superficial velocity on gas hold-up for different particle sizes.

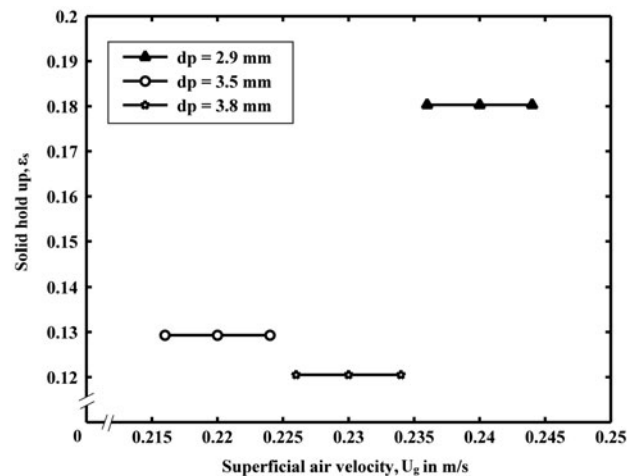


Fig. 14. Effect of superficial velocity on solid hold-up for different particle sizes.

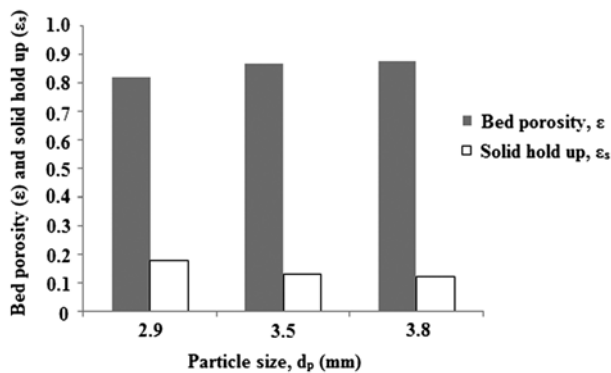


Fig. 15. Effect of media size on fluidized bed porosity and solid hold-up at the optimized superficial air velocity.

3.5. Effect of media size on fluidized bed porosity

Fig. 15 compares the effect of media size on fluidized bed porosity (ϵ) and solid hold-up (ϵ_s) at the optimized superficial air velocity. Smaller media size requires more number of particles for a fixed bed height to reactor volume ratio resulting in higher solid hold-up in the reactor. Fluidized bed porosity is the solid free volume occupied in the reactor and is inversely proportional to solid hold-up and it increases with media size [37].

4. Conclusions

Hydrodynamic characteristic performance of the three phase IFBBR has been studied for the phenol concentration of 1,200 mg/l and fixed bed height ($V_b/V_r=0.20$) of various particle sizes (2.9, 3.5, and 3.6 mm). The superficial gas velocity (U_g) was varied as 0.236, 0.240, and 0.244 m/s for 2.9 mm, 0.216, 0.220, and 0.224 m/s for 3.5 mm, and 0.226, 0.230, and 0.234 m/s for 3.8 mm diameter bioparticles. The influence of operating parameters, such as phase hold-up, aspect ratio, settled bed height, and superficial air velocity on biofilm performance was analyzed. The particle loading was varied in order to determine the effect of phase hold-up on bed homogeneity. The ranges in which particle loading and U_g affect fluidization, and consequently COD reduction, were determined for better biofilm performance characteristics. By varying the diameter of the support particles and the corresponding superficial gas velocities, the optimum U_g for 2.9, 3.5, and 3.8 mm bio particles was found to be 0.240, 0.220, and 0.230 m/s, respectively, for effective degradation of phenol. Complete degradation of phenol was achieved in 32, 48, and 52 h for 2.9, 3.5, and 3.8 mm diameter support particles, respectively. The optimum media size

was found to be 3.5 mm operated with low-superficial velocity resulting in better biofilm performance for effective degradation of phenolic effluent.

Nomenclature

A	—	cross-sectional area of the column, m^2
g_{AVS}	—	mass of bioparticle (in terms of attached volatile solid), g
g_{solid}	—	mass of solid support particle, g
H_s	—	height of settled bed, m
L_f	—	biofilm thickness, μm
M_s	—	mass of solid particles, kg
S	—	substrate concentration, mg/l
V_b	—	volume of settled bed height, m^3
V_r	—	working volume of reactor, m^3
X_f	—	biofilm dry density, kg/m^3
X_{sus}	—	suspended biomass concentration in bulk liquid, mg/l
Z_f	—	aerated liquid level in column after fluidization, m
Z_i	—	initial liquid level in column before aeration, m
ρ_b	—	bioparticle density, kg/m^3
ρ_s	—	density of solid phase (support particles), kg/m^3
ϵ	—	fluidized bed porosity
ϵ_g	—	gas hold-up
ϵ_s	—	solid hold-up
IFBBR	—	inverse fluidized bed biofilm reactor
COD	—	chemical oxygen demand, mg/l

References

- [1] A. Pakuła, E. Bieszkiewicz, H. Boszczyk-Maleszak, R. Mycielski, Biodegradation of phenol by bacterial strains from petroleum-refining wastewater purification plant, *Acta Microbiol. Pol.* 48 (1999) 373–380.
- [2] J.M. Garrido, W.A.J. van Benthum, M.C.M. van Loosdrecht, J.J. Heijnen, Influence of dissolved oxygen concentration on nitrite accumulation in a biofilm airlift suspension reactor, *Biotechnol. Bioeng.* 53 (1997) 167–178.
- [3] L. Tjihuis, M.C.M. van Loosdrecht, J.J. Heijnen, Formation and growth of heterotrophic aerobic biofilms on small suspended particles in airlift reactors, *Biotechnol. Bioeng.* 44 (1994) 595–608.
- [4] Y. Liu, B. Capdeville, Specific activity of nitrifying biofilm in water nitrification process, *Water Res.* 30 (1996) 1645–1650.
- [5] S.Y. Selivanovskaya, A.M. Petrov, K.V. Egorova, R.P. Naumova, Protozoan and metazoan communities treating a simulated petrochemical wastewater in a rotating disc biological reactor, *World J. Microbiol. Biotechnol.* 13 (1997) 511–517.
- [6] B. Rusten, B. Eikebrokk, Y. Ulgenes, E. Lygren, Design and operations of the Kaldnes moving bed biofilm reactors, *Aquacult. Eng.* 34 (2006) 322–331.
- [7] Y. Liu, J.H. Tay, Detachment forces and their influence on the structure and metabolic behavior of biofilm—A review, *World J. Microbiol. Biotechnol.* 17 (2001) 111–117.
- [8] B.E. Rittmann, Comparative performance of biofilm reactor types, *Biotechnol. Bioeng.* 24 (1982) 1341–1370.

- [9] H.T. Chang, B.E. Rittmann, D. Amar, R. Heim, O. Ehlinger, Y. Lesty, Biofilm detachment mechanisms in a liquid-fluidized bed, *Biotechnol. Bioeng.* 38 (1991) 499–506.
- [10] M.C.M. van Loosdrecht, L. Tjihuis, A. Wijdieks, J. Heijnen, L. Tjihuis, J.J. Heijnen, Population distribution in aerobic biofilms on small suspended particles, *Water Sci. Technol.* 31 (1995) 163–171.
- [11] W.K. Kwok, C. Picioreanu, S.L. Ong, M.C.M. van Loosdrecht, W.J. Ng, J.J. Heijnen, Influence of biomass production and detachment forces on biofilm structures in a biofilm airlift suspension reactor, *Biotechnol. Bioeng.* 58 (1998) 400–407.
- [12] C.F. Alves, L.F. Melo, M.J. Vieira, Influence of medium composition on the characteristics of a denitrifying biofilm formed by *Alcaligenes denitrificans* in a fluidised bed reactor, *Process Biochem.* 37 (2002) 837–845.
- [13] A.A. Ulson de Souza, H.L. Brandão, I.M. Zamporlini, H.M. Soares, S.M.D.A. Guelli Ulson de Souza, Application of a fluidized bed bioreactor for cod reduction in textile industry effluents, *Resour. Conserv. Recycl.* 52 (2008) 511–521.
- [14] R. Souza, I.T.L. Bresolin, T.L. Bioni, M.L. Gimenes, B.P. Dias, The performance of a three phase fluidized bed reactor in treatment of waste water with high organic load, *Braz. J. Chem. Eng.* 21 (2004) 219–227.
- [15] S.E. Agarry, B.O. Solomon, Kinetics of batch microbial degradation of phenols by indigenous *Pseudomonas fluorescens*, *Int. J. Environ. Sci. Technol.* 5 (2008) 223–232.
- [16] S. Sabarunisha Begum, K.V. Radha, Hydrodynamic behavior of inverse fluidized bed biofilm reactor for phenol biodegradation using *Pseudomonas fluorescens*, *Korean J. Chem. Eng.* 31 (2014) 436–445.
- [17] W. Sokół, A. Ambaw, B. Woldeyes, Biological wastewater treatment in the inverse fluidised bed reactor, *Chem. Eng. J.* 150 (2009) 63–68.
- [18] L.T. Mulcahy, W.K. Shieh, Fluidization and reactor biomass characteristics of the denitrification fluidized bed biofilm reactor, *Water Res.* 21 (1987) 451–458.
- [19] J. Muller, Disintegration as a key step in sewage sludge treatment, *Water Sci. Technol.* 41 (2000) 123–139.
- [20] L. Nikolov, D. Karamanev, Experimental study of the inverse fluidized bed biofilm reactor, *Can. J. Chem. Eng.* 65 (1987) 214–217.
- [21] L.S. Fan, S.J. Hwang, A. Matsuura, Hydrodynamic behaviour of a draft tube gas–liquid–solid spouted bed, *Chem. Eng. Sci.* 39 (1984) 1677–1688.
- [22] T. Renganathan, K. Krishnaiyah, Prediction of minimum fluidization velocity in two and three phase inverse fluidized beds, *Can. J. Chem. Eng.* 81 (2003) 853–860.
- [23] APHA, Standards Methods for the Examination of Water and Wastewater, 16th ed., American Public Health Association, American Water Works Association, Water Pollution Control Federation, Washington, DC, 1992.
- [24] R.D. Yang, A.E. Humphrey, Dynamic and steady state studies of phenol biodegradation in pure and mixed cultures, *Biotechnol. Bioeng.* 17 (1975) 1211–1235.
- [25] S.E. Agarry, T.O.K. Audu, B.O. Solomon, Substrate inhibition kinetics of phenol degradation by *Pseudomonas fluorescens* from steady state and wash-out data, *Int. J. Environ. Sci. Technol.* 6 (2009) 443–450.
- [26] D. García-Calderón, P. Buffière, R. Moletta, Influence of biomass accumulation on bed expansion characteristics of a down-flow anaerobic fluidized-bed reactor, *Biotechnol. Bioeng.* 57 (1998) 136–144.
- [27] F.K. Rabah, M.F. Dahab, Biofilm and biomass characteristics in high-performance fluidized-bed biofilm reactors, *Water Res.* 38 (2004) 4262–4270.
- [28] T.C. Zhang, P.L. Bishop, Substrate, activity and composition of biofilm, *Water Sci. Technol.* 29 (1994) 335–344.
- [29] H.M. Jena, B.K. Sahoo, G.K. Roy, B.C. Meikap, Characterization of hydrodynamic properties of a gas–liquid–solid three-phase fluidized bed with regular shape spherical glass bead particles, *Chem. Eng. J.* 145 (2008) 50–56.
- [30] A. Ochieng, T. Ogada, W. Sisenda, P. Wambua, Brewery wastewater treatment in a fluidised bed bioreactor, *J. Hazard. Mater.* 90 (2002) 311–321.
- [31] S. Begum, K.V. Radha, Biodegradation kinetic studies on phenol in internal draft tube (inverse fluidized bed) biofilm reactor using *Pseudomonas fluorescens*: Performance evaluation of biofilm and biomass characteristics, *Biorem. J.* 17 (2013) 264–277.
- [32] Y. Liu, J.H. Tay, The essential role of hydrodynamic shear force in the formation of biofilm and granular sludge, *Water Res.* 36 (2002) 1653–1665.
- [33] H. Beyenal, A. Tanyolaç, The effects of biofilm characteristics on the external mass transfer coefficient in a differential fluidized bed biofilm reactor, *Biochem. Eng. J.* 1 (1998) 53–61.
- [34] A. Gjaltema, M.C.M. van Loosdrecht, J.J. Heijnen, Abrasion of suspended biofilm pellets in airlift reactors: Effect of particle size, *Biotechnol. Bioeng.* 55 (1997) 206–215.
- [35] D. Zhou, X.T. Bi, S. Dong, Contribution of hydrodynamic characteristics on the performance of an aerobic biofilm conical fluidized bed, *Water Sci. Technol.* 63 (2011) 1160–1167.
- [36] H.D. Han, W. Lee, Y.K. Kim, J.L. Kwon, H.S. Choi, Y. Kang, S.D. Kim, Phase hold-up and critical fluidization velocity in a three-phase inverse fluidized bed, *Korean J. Chem. Eng.* 20 (2003) 163–168.
- [37] C. Nicolella, M.C.M. van Loosdrecht, R.G.M. van der Lans, J.J. Heijnen, Hydrodynamic characteristics and gas–liquid mass transfer in a biofilm airlift suspension reactor, *Biotechnol. Bioeng.* 60 (1998) 627–635.